Evaluation of Failure Parameters in Composite Structures by Component-Wise Approach

E. Carrera*, M. Maiarú†, and M. Petrolo‡

Department of Mechanical and Aerospace Engineering, Politecnico di Torino, Torino, Italy

This paper proposes a new approach for the FE analysis of composite structures by means of 1D refined models that have been derived in the framework of the Carrera Unified Formulation (CUF). CUF provides hierarchical higher-order structural models with arbitrary expansion orders. Taylor- and Lagrange-type polynomials were used to interpolate the displacement field over the element cross-section. The proposed new approach, referred to as Composite-Wise (CW), is able to provide stress and strain fields with solid-like accuracy and very low computational cost. Within the CW approach, different scale components (fiber, matrix, laminae and laminates) can be simultaneously considered in the same structural model. Failure analyses are conducted by implementing well-known failure criteria. Furthermore, an integral evaluation of failure parameters is introduced to determine critical portion of the structure where failure could take place. Results are provided to show the enhaced capability of the present formulation in the failure analysis of fiber-reinforced composite structures by the detection of detailed displacement/stress fields with reduced computational cost.

I. Introduction

Composites provide significant advantages in performance, efficiency and costs; thanks to these features, the application of composite structures is increasing in many engineering fields. Despite the great benefits that they provide, there are issues to be addressed, e.g. failure mechanisms, to enhance the design of composite structures. Composite structures are characterized by different length scales; referring to fiber reinforced composites, the involved scales can be the micro- (fiber/matrix), meso- (lamina) and macro-scale (whole laminate). The proper modeling of these scales and their interactions is of primary importance to detect reliable stress fields and to evaluate the structural integrity of a composite structure. Many techniques are available to compute accurate stress/strain fields in a composite structure, some of these techniques are briefly discussed hereafter.

A multi-scale approach is required when micro- and macro-scales are accounted for. An overview about the available multiscale techniques has been provided by Lu and Kaxiras.[1] When also the nano-scale is taken into account, a possible approach is based on the use of the molecular dynamics at the nano-scale level, the Representative Volume Elements at micro-level and structural elements at the macro-scale. The Generalized Method of Cell (GMC)[2,3,4] developed by Paley and Aboudi is an important tool in the multiscale framework. Analysis by means of 1D and 2D components are performed in the framework of FE (Finite Element) method, a refined technique consists in using 3D solid finite elements. These elements can be employed to discretize single components (fibers and matrices) or to directly model the layer of a laminated structure. That is, fibers and matrices can be modeled as being independent elements or they can be homogenized to compute layer properties. Due to the limitations of the aspect ratio of 3D elements and to the high number of layers used in real applications, computational costs of a solid model could be prohibitive. Classical theories which are known for traditional beam (1D) and plate/shell (2D) structures had been improved for their application to laminates. Numerous contributions have been presented in the literature regarding higher-order models,[5,6] Zig-zag theories[7,8,9,10] and Layer-Wise (LW) approaches.[11,12,13] So-called *global-local* approaches have also been developed by exploiting

*Professor,Department of Mechanical and Aerospace Engineering, Politecnico di Torino, Corso Duca degli Abruzzi, 24, 10129 Torino, Italy.

†PhD Student, Department of Mechanical and Aerospace Engineering, Politecnico di Torino.

‡PhD, Department of Mechanical and Aerospace Engineering, Politecnico di Torino.

the superposition of Equivalent Single Layer (ESL) and Layer-Wise (LW) models,[14] or by using the Arlequin method to combine higher- and lower-order theories.[15,16,17] The method proposed in this paper, referred to as Component-wise (CW), is based on the 1D Carrera Unified Formulation (CUF).[18] 'Component-wise' means that each typical component of a composite structure (i.e. layers, fibers and matrices) can be separately modeled by means of a single formulation. Moreover, in a given model, different scale components can be used simultaneously, that is, homogenized laminates or laminae can be interfaced with fibers and matrices as shown in Figure 1. This feature allows to tune the model capabilities by choosing in which portion of the structure a more detailed model has to be used or, in other words, it make possible obtain progressively refined models up to the fiber and matrix dimensions. Furthermore, the order of the structural model can be set as input. Because of their complexity, dam-

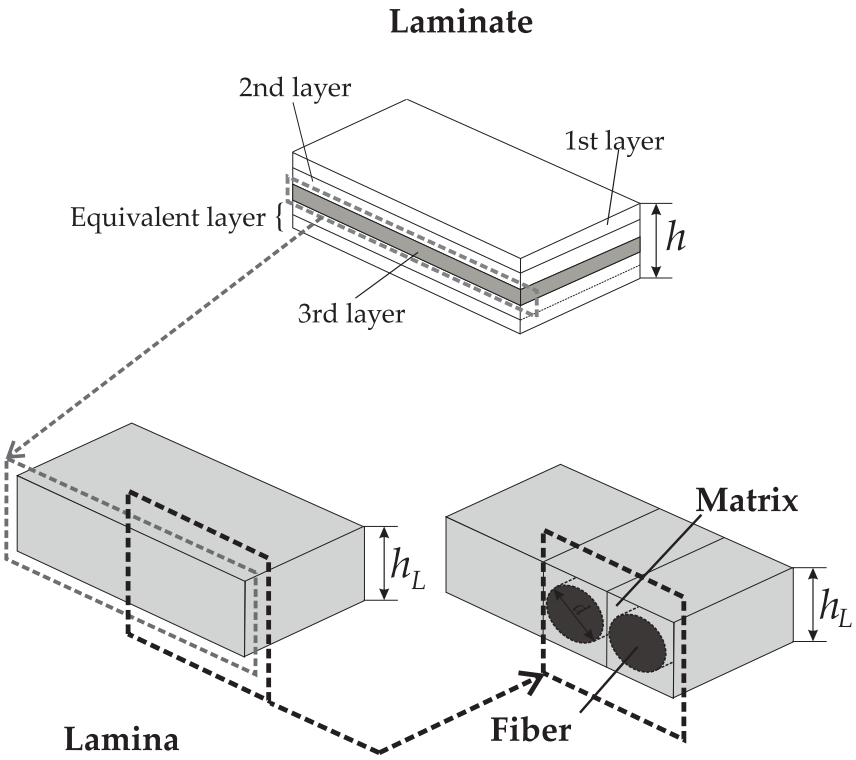

Figure 1. Component-Wise approach to simultaneously model layers, fibers and matrices

ages and failure mechanisms in composites are very different from those of metallic materials. They are heavily affected by many parameters such as geometry, lay-up and boundary conditions. A wide number of criteria exist to predict the occurrence of failure in fiber-reinforced composite materials. They can be classified depending on the stress/strain components that are considered. A brief overview of the most important two-dimensional failure criteria for anisotropic materials is given in Nali and Carrera,[19] while Orifici et Al.[20] consider a 3D stress/strain state. The World Wide Failure Exercise (WWFE) provided a comprehensive assessment of the methods to predict the failure initiation in fiber-reiforced composites. From the WWFE, Puck failure criterion[21] has emerged as the most effective. Inspired by Puck's assumptions, NASA Langley Research Centre has formulated some improved criteria in 2D- and 3D-state of stress, respectively LaRC03[22] and LaRC04.[23]

Three different structural models are analyzed in this work. A homogeneous cantilever beam is proposed as preliminary assessment, a solid model is employed to validate results. A single fiber-matrix cell is then considered to display the integral approach capabilities. Last, a cross-ply symmetric laminated [0/90/0] beam is taken into account to assess the proposed approach for complex structural configurations. Results are evaluated in terms of strain energy and Failure Indexes according to two well known criteria. This paper is organized as follows: a brief theoretical introduction to the present formulation is given in Section II, the theoretical background of the CUF formulation is briefly shown in Sections III and IV. An overview about the CW approach for the evaluation of integral parameters is given in section V and numerical examples are carried out in Section VI. Main conclusions

are drawn in Section VII.

II. CUF 1D Formulation

In the coordinate frame shown in Figure 2, the displacement vector is defined as

$$\mathbf{u}(x,y,z) = \left\{ \begin{array}{ccc} u_x & u_y & u_z \end{array} \right\}^T \tag{1}$$

Stress, $\boldsymbol{\sigma}$, and strain, $\boldsymbol{\epsilon}$, components are grouped as follows:

$$\boldsymbol{\sigma}_p = \left\{ \begin{array}{cccccc} \sigma_{xx} & \sigma_{yy} & \sigma_{zz} & \sigma_{xy} & \sigma_{xz} & \sigma_{yz} \end{array} \right\}^T, \boldsymbol{\epsilon}_p = \left\{ \begin{array}{cccccc} \epsilon_{xx} & \epsilon_{yy} & \epsilon_{zz} & \epsilon_{xy} & \epsilon_{xz} & \epsilon_{yz} \end{array} \right\}^T \tag{2}$$

Linear strain-displacement relations are used,

$$\boldsymbol{\epsilon} = \boldsymbol{D}\mathbf{u} = (\boldsymbol{D}_y + \boldsymbol{D}_\Omega)\mathbf{u} \tag{3}$$

where

$$\boldsymbol{D} = \begin{bmatrix} \frac{\partial}{\partial x} & 0 & 0 \\ 0 & \frac{\partial}{\partial y} & 0 \\ 0 & 0 & \frac{\partial}{\partial z} \\ \frac{\partial}{\partial y} & \frac{\partial}{\partial x} & 0 \\ \frac{\partial}{\partial z} & 0 & \frac{\partial}{\partial x} \\ 0 & \frac{\partial}{\partial z} & \frac{\partial}{\partial y} \end{bmatrix} = \begin{bmatrix} \frac{\partial}{\partial x} & 0 & 0 \\ 0 & 0 & 0 \\ 0 & 0 & \frac{\partial}{\partial z} \\ 0 & \frac{\partial}{\partial x} & 0 \\ \frac{\partial}{\partial z} & 0 & \frac{\partial}{\partial x} \\ 0 & \frac{\partial}{\partial z} & 0 \end{bmatrix} + \begin{bmatrix} 0 & 0 & 0 \\ 0 & \frac{\partial}{\partial y} & 0 \\ 0 & 0 & 0 \\ \frac{\partial}{\partial y} & 0 & 0 \\ 0 & 0 & 0 \\ 0 & 0 & \frac{\partial}{\partial y} \end{bmatrix} = [\boldsymbol{D}_\Omega] + [\boldsymbol{D}_y] \tag{4}$$

Constitutive laws are exploited to obtain stress components,

$$\boldsymbol{\sigma} = \boldsymbol{C}\boldsymbol{\epsilon} \tag{5}$$

The components of $\boldsymbol{C}$ are the material coefficients whose explicit expressions are not reported here for the sake of brevity, they can be found in Reddy.[24]

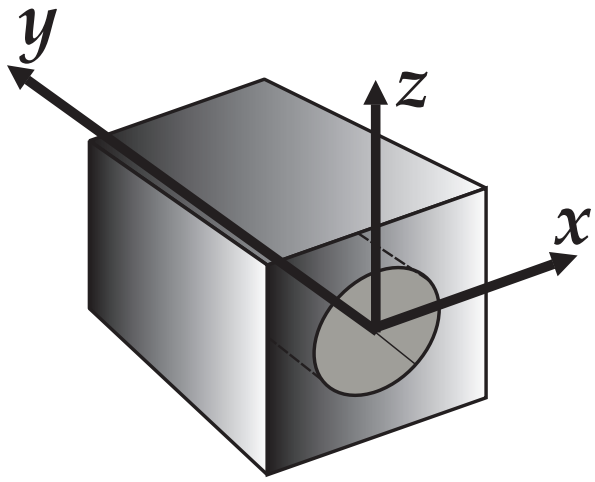

Figure 2. Coordinate frame.

III. Hierarchical Higher-Order Models, TE and LE classes

In the CUF framework, the displacement field can be approximated through the expansion of generic functions, F_τ,

$$\mathbf{u} = F_\tau \mathbf{u}_\tau, \qquad \tau = 1, 2, ..., M \tag{6}$$

where F_τ vary above the cross-section. $\mathbf{u}_\tau$ is the displacement vector and M stands for the number of terms of the expansion. According to the Einstein notation, the repeated subscript, τ, indicates summation. The choice of F_τ determines the adopted class of 1D CUF model.
The Taylor Expansion class (TE) is based on Taylor-like polynomial expansions, $x^i\ z^j$, of the displacement field above the cross- section of the structure (i and j are positive integers). The order N of the expansion is arbitrary and is set as an input of the analysis. A convergence study is usually needed to choose N for a given structural problem. For example, the second-order model, $N = 2$, has the following kinematic model:

$$\begin{aligned} u_x &= u_{x_1} + x\ u_{x_2} + z\ u_{x_3} + x^2\ u_{x_4} + xz\ u_{x_5} + z^2\ u_{x_6} \\ u_y &= u_{y_1} + x\ u_{y_2} + z\ u_{y_3} + x^2\ u_{y_4} + xz\ u_{y_5} + z^2\ u_{y_6} \\ u_z &= u_{z_1} + x\ u_{z_2} + z\ u_{z_3} + x^2\ u_{z_4} + xz\ u_{z_5} + z^2\ u_{z_6} \end{aligned} \tag{7}$$

The 1D model described by Eqs. 7 has 18 generalized displacement variables; three constant, six linear, and nine parabolic terms. Classical beam theories, Euler-Bernoulli (EBBT) and Timoshenko (TBT), can be obtained as particular cases of the $N = 1$ model, as shown in Carrera at Al.[25]
The Lagrange Expansion class (LE) exploits Lagrange polynomials to build 1D refined models. The isoparametric formulation is exploited to deal with arbitrary shaped geometries. The L9 interpolation polynomials are given by Oñate[26]

$$F_\tau = \tfrac{1}{4}(r^2 + r\ r_\tau)(s^2 + s\ s_\tau) \qquad \tau = 1, 3, 5, 7$$

$$F_\tau = \tfrac{1}{2}s_\tau^2(s^2 + s\ s_\tau)(1 - r^2) + \tfrac{1}{2}r_\tau^2(r^2 + r\ r_\tau)(1 - s^2) \qquad \tau = 2, 4, 6, 8 \tag{8}$$

$$F_\tau = (1 - r^2)(1 - s^2) \qquad \tau = 9$$

where r and s range from -1 to $+1$ and r_τ and s_τ are the natural coordinates of the interpolation points above the cross-section. The displacement field given by a L9 element is

$$\begin{aligned} u_x &= F_1\ u_{x_1} + F_2\ u_{x_2} + F_3\ u_{x_3} + F_4\ u_{x_4} + F_5\ u_{x_5} + F_6\ u_{x_6} + F_7\ u_{x_7} + F_8\ u_{x_8} + F_9\ u_{x_9} \\ u_y &= F_1\ u_{y_1} + F_2\ u_{y_2} + F_3\ u_{y_3} + F_4\ u_{y_4} + F_5\ u_{y_5} + F_6\ u_{y_6} + F_7\ u_{y_7} + F_8\ u_{y_8} + F_9\ u_{y_9} \\ u_z &= F_1\ u_{z_1} + F_2\ u_{z_2} + F_3\ u_{z_3} + F_4\ u_{z_4} + F_5\ u_{z_5} + F_6\ u_{z_6} + F_7\ u_{z_7} + F_8\ u_{z_8} + F_9\ u_{z_9} \end{aligned} \tag{9}$$

where $u_{x_1}, ..., u_{z_9}$ are the displacement variables of the problem and they represent the pure displacement components of each of the nine points of the L9 element. This means that LE models provide elements that have only pure displacement variables. L6 models are obtained in the same manner, the explicit expression of these polynomials are not reported here, they can be found in Oñate.[26]

IV. FE Formulation and the Fundamental Nucleus

The FE approach was herein adopted to discretize the structure along the y-axis, this process was conducted via a classical finite element methodology based on the Principle of Virtual Displacements. The shape functions, N_i, and the nodal displacement vector, $\mathbf{q}_{\tau i}$, are used and the displacement vector becomes

$$\mathbf{u}(x, y, z) = N_i(y)F_\tau(x, z)\mathbf{q}_{\tau i}, \qquad i = 1, 2, ..., K \tag{10}$$

with

$$\mathbf{q}_{\tau i} = \left\{ \begin{array}{ccc} q_{u_{x_{\tau i}}} & q_{u_{y_{\tau i}}} & q_{u_{z_{\tau i}}} \end{array} \right\}^T \tag{11}$$

where K is the number of the nodes on the element. For the sake of brevity, the explicit forms of the shape functions, N_i, are not reported here, they can be found in Bathe.[27] Elements with 4 nodes, here denoted as B4, were used in this paper, that is, a cubic approximation along the y axis was adopted.
The stiffness matrix is obtained via the Principle of Virtual Displacements in the form of the fundamental nucleus. The explicit forms of the 9 components of $K_{ij\tau s}$ are not reported here, they can be found in Carrera and Petrolo.[13]
The strain energy is obtained via the Principle of Virtual Displacements

$$\delta L_{int} = \delta L_{ext} \tag{12}$$

where

$$\delta L_{int} = \delta q_{\tau i}^T K_{ij\tau s} q_{\tau i} \tag{13}$$

V. The CW approach for the evaluation of integral quantities

The CW approach allows the modelling of a fiber-reinforced composite structure up to the component scale. Previous works have evidenced CW enhanced structural capabilities to detect accurate stress/strain fields in the matrix, fibers, layers and interfaces of composite layered structures with low computational costs. Numerical results on different structural problems can be found in Carrera et Al.,[18,28] where comparisons with solid models have been provided. The present work proposes to exploit this approach to evaluate integral quantities to identify potential critical areas of a composite structure. In composite structures, failure can occurs due to fiber or matrix collapse, debonding or delamination. To determine where failure occurs, integral quantities can be evaluated in subdomains that can be lines, areas or volumes of the components or at lamina/fiber-matrix interfaces. After a preliminary analysis at the macroscale level, the model capabilities can be tuned by choosing in which portion of the structure a more detailed model has to be used. In other words, detailed models can be progressively obtained up to the fiber and matrix subvolume dimensions to identify which part of the structure is working in the most critical conditions. Failure index offers a punctual evaluation of the criticality in a given structure. To overcome the puntual evaluation the CW integral approach is applied to evaluate a failure parameter related to subvolumes. Results are given in terms of "failure index density" FI_i^* where, FI_i^* is a function calculated as reported in eq.14 for a i-th subvolume.

$$FI_i^* = \frac{\int_{V_i} FI dV_i}{V_i} \tag{14}$$

Given a criterion, the corresponding FI is integrated in the subvolume dV_i and then normalized for the correspondind volume V_i. In order to obtain an evaluation on larger portions of the structure, subvolumes are combined and a further index is proposed in eq. 15 where the FI_i^* of each subvolume is summed and then normalised with respect to $NVol$ that is the total number of summed subvolumes.

$$FI^* = \frac{\sum_{k=1}^{NVol} \frac{\int_{V_i} FI dV_i}{V_i}}{NVol} \tag{15}$$

VI. Numerical results

Numerical examples have been carried out for different structural models. A homogeneous beam was considered as first assessment. Solid comparisons were provided. Then, a single fiber-matrix cell was considered. Last, a multilayered beam was considered with a fiber/matrix cell included in the third layer. For the homogeneous case study, in order to validate the estimation of the integral parameter, results are compared with those of a solid model built through 1080 20-node hexaedron elements. In Figure 3 the two employed meshes are provided respectively for the CW model and for the solid model, one of the ten subvolumes taken into account is highlighted by the red line. The CW mesh is obtained through one nine-points (L9) element on the cross-section and 30 B3 elements along the y-axis. The structure is clamped at one end and four bending forces are applied at the free-tip, F = 0.025 N. In Table 1 results are shown in terms of strain energy, the first column provides CW model results while in the second column solid results are reported. Results show that for each subvolumes the strain energy can be evaluated with solid like accuracy with a reduced computational cost. In fact, the last row in Table 1 shows that CW approach has almost 3 times less DOFs.

Through a further subdivision in 30 subvolumes the local effect of the loading can be seen in Figure 4 where the strain energy distribution along the beam axis is depicted. In the CW approach the simplest structural layout is a fiber/matrix cell. Figure 5 provides a graphic description of a possible modeling refinement for the single cell case study. A typical strategy can be based on a preliminary volume subdivision at macroscale. Where deemed appropriate, components can be identified and finer subvolume distributions can be considered. Fiber and matrix volumes are evaluated with their own properties. The analyzed cell is square with side h = 0.1 mm, and L/h = 10 where L is the longitudinal length of the structure. The fiber diameter is d = 0.08 mm. The mesh is obtained by means of 10 B3 elements along the y-axis and 20 nine-point (L9) elements on the cross-section. Fiber and matrix material properties are shown in Table 2. For each material, failure coefficients are reported. The subscripts T and C denote respectively the limit value in the case of tension and compression. The structure is clamped at y = 0. Two loading configurations are analyzed as shown in Figure 6. In a first case study, four bending force are locally applied on the matrix at the cell corners, F = 0.025 N. Then, in a second case two loading forces, F = 0.05 N, are applied at [0, L, h/2] and [h, L, h/2]. For the evaluation of the integral quantities

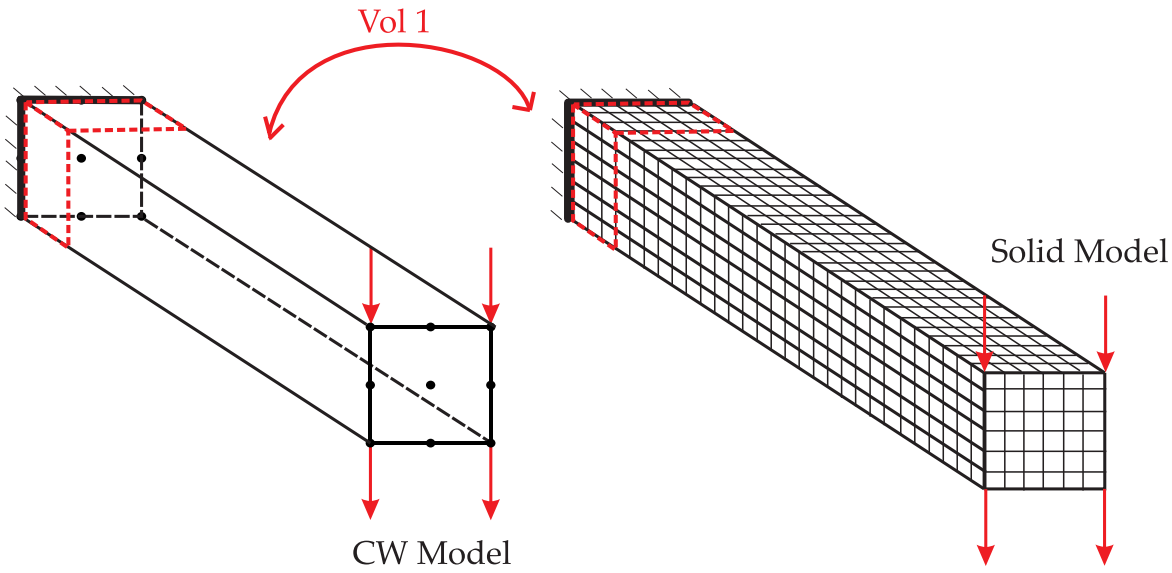

Figure 3. CW and Solid Models for the homogeneous assessment.

	E_i mJ	
Vol	CW	Solid
	$\times 10^4$	
1	1.030	1.023
	E $\times 10^5$	
2	8.529	8.535
3	6.648	6.651
4	5.002	5.006
5	3.592	3.595
6	2.416	2.420
7	1.476	1.479
	$\times 10^6$	
8	7.703	7.738
9	3.000	3.036
10	1.301	1.470
	E $\times 10^4$ mJ	
	3.917	3.914
	DOFs	
	1647	4557

Table 1. Strain energy distribution in homogeneous beam subvolumes.

two main subvolumes of the whole structure are considered as depicted in Figure 7. Results of this preliminary investigation are provided in Table 3 in terms of the total strain energy E, axial strain energy E_{ax} and shear strain energy E_s.

Furthermore, the strain energy of each subvolume, E_i, is normalized with respect to the strain energy of the whole model, E. Axial ($E_{ax,i}$) and shear ($E_{s,i}$) strain energies respectively normalized to the axial E_{ax} and the

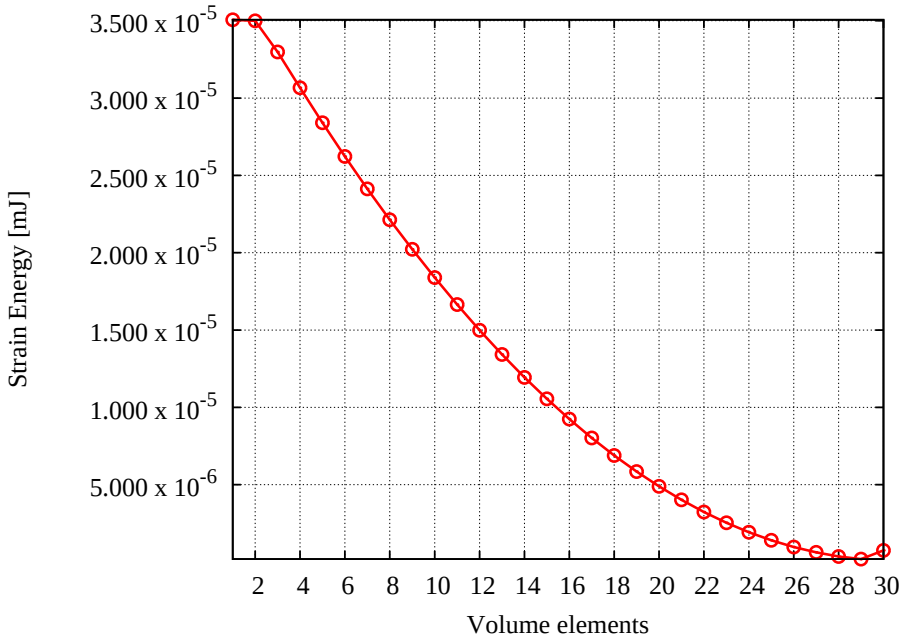

Figure 4. Strain energy distribution along the y-axis.

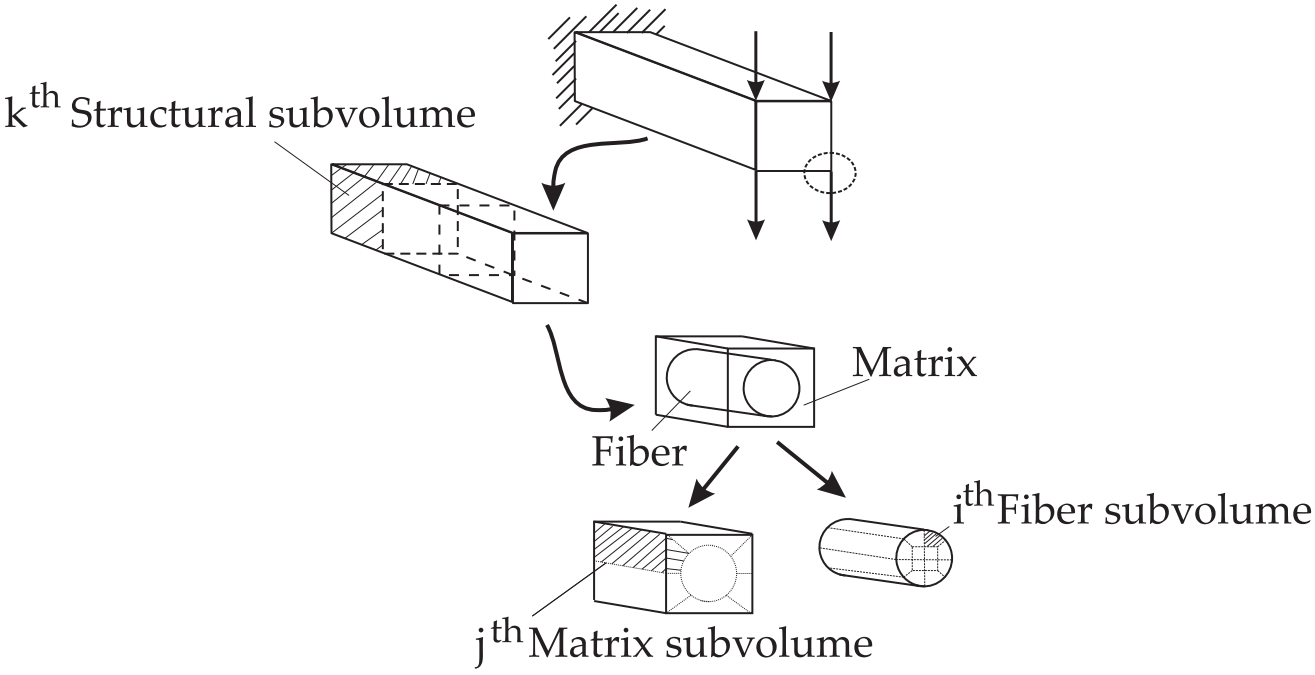

Figure 5. Component-Wise approach for volume evaluations.

shear E_s strain energy of the whole structure are also take into account. This preliminary analysis shows that the main part of the total and axial strain energy of the cell due to the bending are localized around the clamp, while for the the shear strain energy is around the free tip while for the torsion load the main part of the energy is absorbed by the second subvolume. Then, a further subvolume distribution is analyzed, five parts of the structure are considered as depicted in Figure 7.

In this second volume distribution, numerical results show that $E_{i,max}$ and $E_{ax,max}$ are in the first subvolume,

	Homogeneous	Fiber	Matrix
Material Properties			
E [GPa]	127.6	250.6	3.252
ν [-]	0.3	0.2456	0.355
Failure Coefficients			
Maximum Stress [MPa]			
X^T	1730	3398.1	66.5
X^C	1045	2052.6	255
S^L	95.1	186.8	74

Table 2. Material properties and failure coefficients.

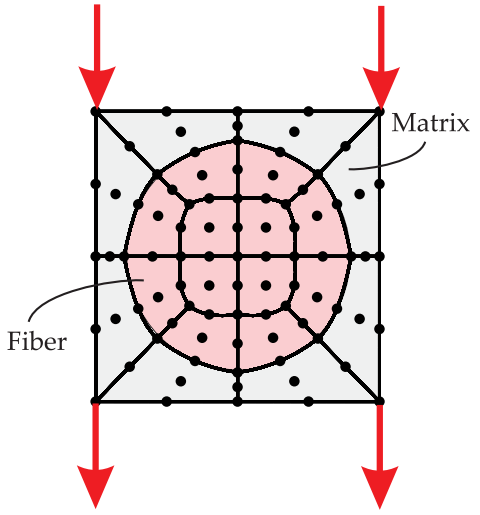

(a) Bending loading case

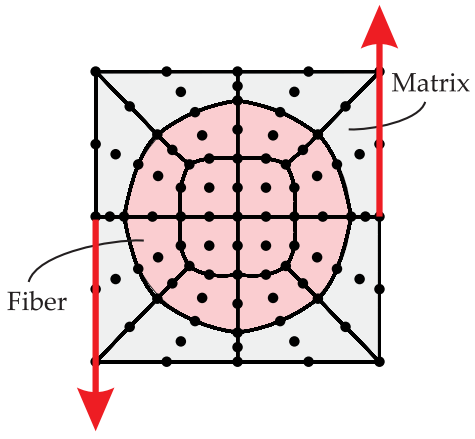

(b) Torsion loading case

Figure 6. Loading configurations.

while $E_{s,max}$ is in the fifth subvolume for the bending load. For the torsion case the fifth subvolume appear to be the most stressed. Furthermore, CW approach is able to distinguish the component strain energies to determine what is the contribution given by the fiber and by the matrix. In Table 4 results are shown for the bending load. The superscrits "f" and "m" respectively refer to fiber and matrix. CW approach shows that in this load

	Bending			Torsion	
Vol	E_i/E	$E_{ax,i}/E_{ax}$	$E_{s,i}/E_s$	E_i/E	$E_{s,i}/E_s$
1/2	**0.846**	**0.874**	0.308	0.138	0.415
2/2	0.154	0.126	**0.692**	**0.862**	**0.585**
1/5	**0.469**	**0.484**	0.177	0.055	0.168
2/5	0.289	0.298	0.089	0.055	0.166
3/5	0.149	0.153	0.082	0.055	0.163
4/5	0.055	0.056	0.083	0.056	0.169
5/5	0.038	0.008	**0.568**	**0.778**	**0.334**
	E mJ	E_{ax} mJ	E_s mJ	E mJ	E_s mJ
	3.448×10^3	3.331×10^3	3.257×10^5	1.150×10^4	3.775×10^5

Table 3. Strain Energy in beam subvolumes.

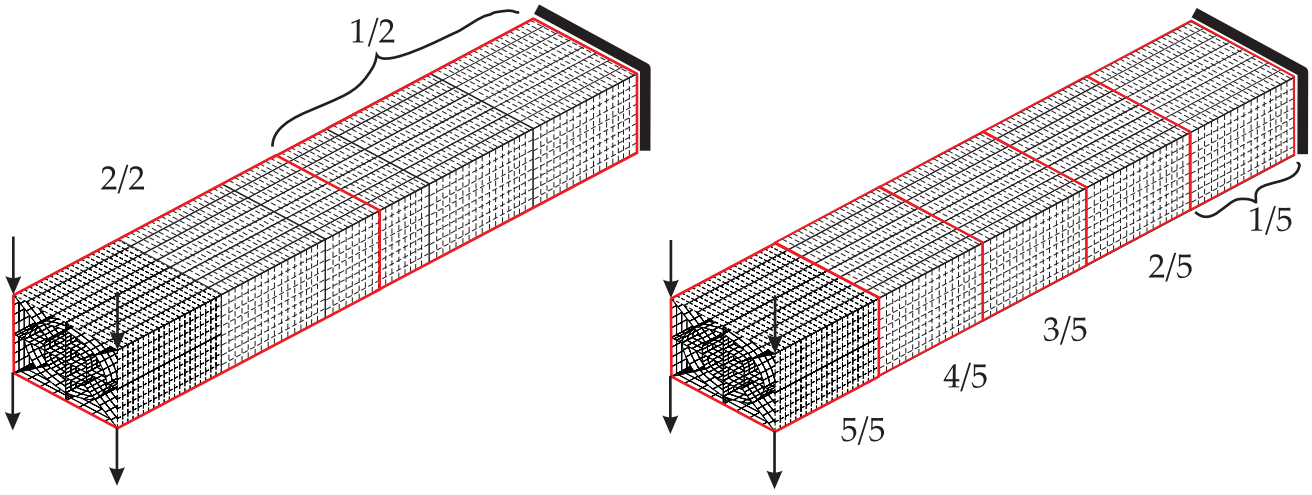

Figure 7. Subvolume distributions.

configuration, the main axial strain energy is absorbed by the fiber while the matrix mainly absorbs the shear strain energy. Table 5 reports results for the torsion loading case.

For both cases, in the last fifth (5/5) it is possible to detect the local effect on the matrix due to the loading. Focusing on the sixteen subvolumes shown in Figure 8, the strain energy at the microscale can be evaluated. Table 6 reports that the bending loading has more effect on the matrix subvolumes 9-16 while the torsion loading affects principally the subvolumes 11-12,15-16.

Single cell: bending						
	Fiber			Matrix		
Vol	$E^f_{,i}/E^f$	$E^f_{ax,i}/E^f_{ax}$	$E^f_{s,i}/E^f_s$	$E^m_{,i}/E^m$	$E^m_{ax,i}/E^m_{ax}$	$E^m_{s,i}/E^m$
1/2	**0.873**	**0.874**	**0.591**	**0.509**	**0.872**	0.046
2/2	0.127	0.126	0.409	0.491	0.128	**0.954**
1/5	**0.483**	**0.484**	**0.326**	**0.275**	**0.488**	0.039
2/5	0.298	0.298	0.180	0.171	0.293	0.005
3/5	0.153	0.153	0.167	0.088	0.151	0.004
4/5	0.057	0.056	0.164	0.033	0.056	0.008
5/5	0.009	0.008	0.162	0.423	0.012	**0.945**
	E^f mJ	E^f_{ax} mJ	E^f_s mJ	E^m mJ	E^m_{ax} mJ	E^m_s mJ
	3.201×10^3	3.186×10^3	1.569×10^5	2.468×10^4	1.449×10^4	1.688×10^5

Table 4. Strain Energy in fiber and matrix subvolumes.

Single cell: torsion				
	Fiber		Matrix	
Vol	$E^f_{,i}/E^f$	$E^f_{s,i}/E^f_s$	$E^m_{,i}/E^m$	$E^m_{s,i}/E^m_s$
1/2	0.501	0.506	0.006	0.042
2/2	0.499	0.494	**0.994**	**0.958**
1/5	0.200	0.202	0.002	0.028
2/5	0.200	0.203	0.002	0.014
3/5	0.200	0.203	0.002	0.000
4/5	0.200	0.202	0.003	0.032
5/5	0.199	0.190	**0.989**	**0.925**
	E^f mJ	E^f_s mJ	E^m mJ	E^m_s mJ
	3.069×10^5	3.035×10^5	8.436×10^5	7.399×10^6

Table 5. Strain Energy in fiber and matrix subvolumes.

On the basis of the stress and strain distribution well known criteria are usually employed to detect the failure initiation. The criteria identify an index, FI, referred to as Failure Index, that becomes the parameter that determines the failure initiation. Points in which the index becomes greater or equal to one indicate the failure. In this work two failure criteria are employed: the Maximum Stress (MS) and Tsai-Wu (TW) criteria. Failure index distributions for both criteria at clamped cross-section, are shown in Figure 9 for the bending case study where, failure occurs in the bottom portion of the fiber. Results, for both the loading case studies, are given in terms of "failure index density" FI^* in Table 7. The failure parameter FI^* is evaluated on fiber and matrix, approximations introduced by the homogenization theories are avoided.

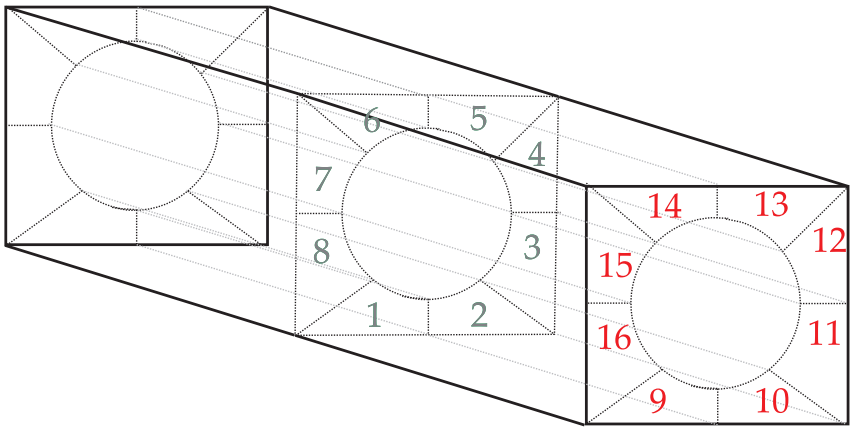

Figure 8. Matrix subvolumes near the free tip.

	Bending		Torsion	
Vol ID	$E^m_{,j}/E^{m*}$	$E^m_{s,j}/E^{m*}$	$E^m_{,j}/E^{m*}$	$E^m_{s,j}/E^{m*}$
1	0.004	0.006	0.000	0.003
2	0.004	0.006	0.000	0.003
3	0.003	0.003	0.006	0.014
4	0.003	0.003	0.006	0.014
5	0.004	0.006	0.000	0.003
6	0.004	0.006	0.000	0.003
7	0.003	0.003	0.006	0.014
8	0.003	0.003	0.006	0.014
9	0.079	0.123	0.003	0.013
10	0.079	0.123	0.003	0.013
11	0.164	0.117	0.241	0.220
12	0.164	0.117	0.241	0.220
13	0.079	0.123	0.003	0.013
14	0.079	0.123	0.003	0.013
15	0.164	0.117	0.241	0.220
16	0.164	0.117	0.241	0.220

Table 6. Local Effect on matrix due to the bending loads.

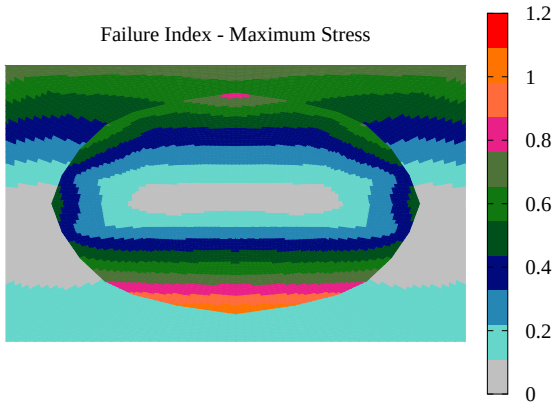

(a)

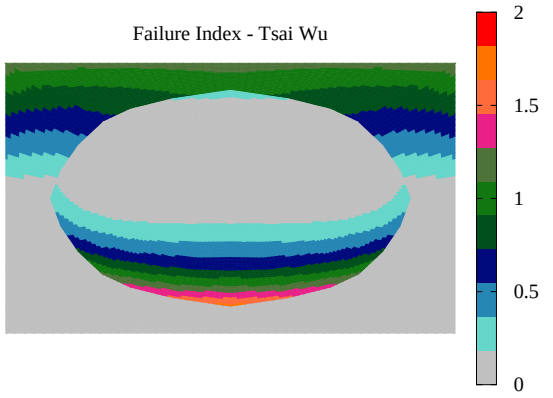

(b)

Figure 9. Maximum Stress (MS) and Tsai-Wu (TW) Failure indexes over the single cell clamped cross-section under bending loading.

The CW approach appears to be attractive in the perspective of a detailed analysis of more complex structural configurations. Cells can be opportunely included in order to refine the model in areas that were considered critical following preliminary analyses. As previously shown in Figure 5, subvolumes can be an entire subdomain of the structure (i.e. a third of the cell) or, as depicted in Figure 10 for more complex configurations, entire laminae, a whole fiber or an entire portion of matrix.
The structural analysis of a cantilever laminated beam is herein proposed. Stacking sequence of the plies is [0/90/0]. The geometry of this model is described in Figure 10. The height (h) and the width (b) are equal to 0.6 mm and 0.8 mm, respectively. L/h = 10. For each layer h_i = 0.2 mm. A fiber/matrix cell is modeled as having a geometry of the previous analyzed cell. The mesh is obtained by means of 15 B3 elements along the y-axis and 41 L9 elements on the cross-section as depicted in Figure 12. Lamina, fiber and matrix material properties are shown in Table 2. The structure is clamped at y = 0. Two loading configurations are analyzed as shown in Figure 11 and Figure 12. In a first case study, a bending force is locally applied on the center of the second lamina, F = 0.5 N. Then, in a second case four torsion forces, F = 1 N, are applied as shown in Figure 11.

In this structural configuration, the three layers are chosen as main subvolumes. Results are shown in Table 8 in terms of strain energy. It is possible to observe that in the bending load configuration the first and the third lamina absorb the main part of the axial strain energy while the second absorb the 77,2% of the shear strain energy. Torsion loading determines a mainly equal redistribution of the strain energy. Furthermore it is possible to evaluate the strain energy absorbed by the cell included. Table 9 shows the total amount of energy absorbed,

	Bending				Torsion			
	Fiber		Matrix		Fiber		Matrix	
Vol	FI* TW	FI* MS	FI* TW	FI* MS	FI* TW	FI* MS	FI* TW	FI* MS
	0.070	0.124	0.010	0.050	0.073	0.095	0.008	0.009
1/2	0.097	0.163	0.006	0.063	0.074	0.096	0.000	0.003
2/2	0.044	0.086	0.014	0.036	0.073	0.094	0.016	0.014
1/5	0.129	0.190	0.007	0.077	0.074	0.096	0.000	0.003
2/5	0.082	0.153	0.006	0.058	0.074	0.096	0.000	0.003
3/5	0.058	0.119	0.003	0.042	0.074	0.096	0.000	0.003
4/5	0.043	0.089	0.001	0.025	0.074	0.096	0.000	0.004
5/5	0.039	0.069	0.032	0.046	0.072	0.092	0.041	0.029

Table 7. Failure index integrated over the subvolumes normalized with respect to the number of subvolumes.

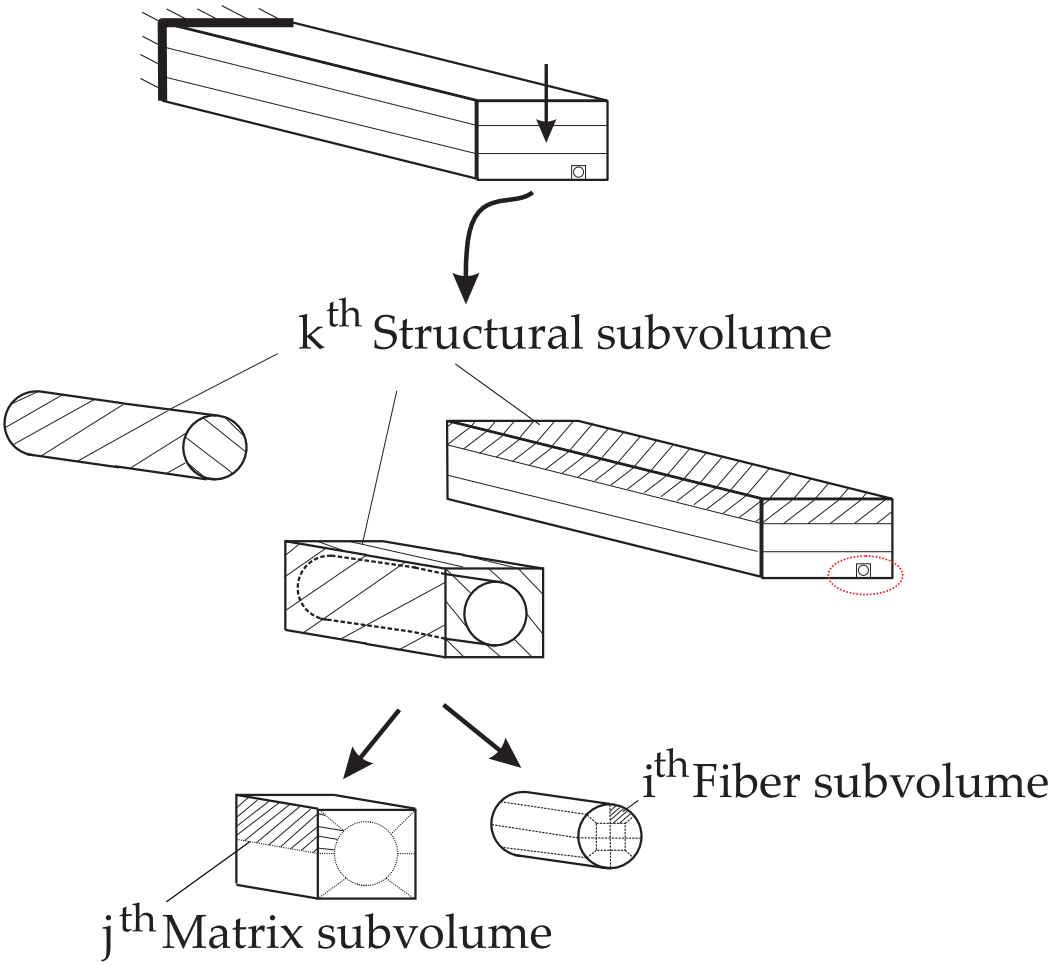

Figure 10. Component-Wise approach for volume evaluations.

and the total, axial and strain energy normalized with respect to the total, axial and shear strain energy of the

	Bending			Torsion		
Lamina	E_i/E	$E_{ax,i}/E_{ax}$	$E_{s,i}/E_s$	E_i/E	$E_{ax,i}/E_{ax}$	$E_{s,i}/E_s$
1	0.451	0.499	0.116	0.353	0.508	0.319
2	0.099	0.003	0.772	0.302	0.021	0.358
3	0.450	0.499	0.113	0.345	0.471	0.323
	E [mJ]	E_{ax} [mJ]	E_s [mJ]	E [mJ]	E_{ax} [mJ]	E_s [mJ]
Laminate	5.797×10^1	5.077×10^1	6.833×10^2	7.330×10^2	9.671×10^4	6.071×10^2

Table 8. Strain energy distribution in a laminate beam under bending F = 0.5 N and torsion F = 1 N loads.

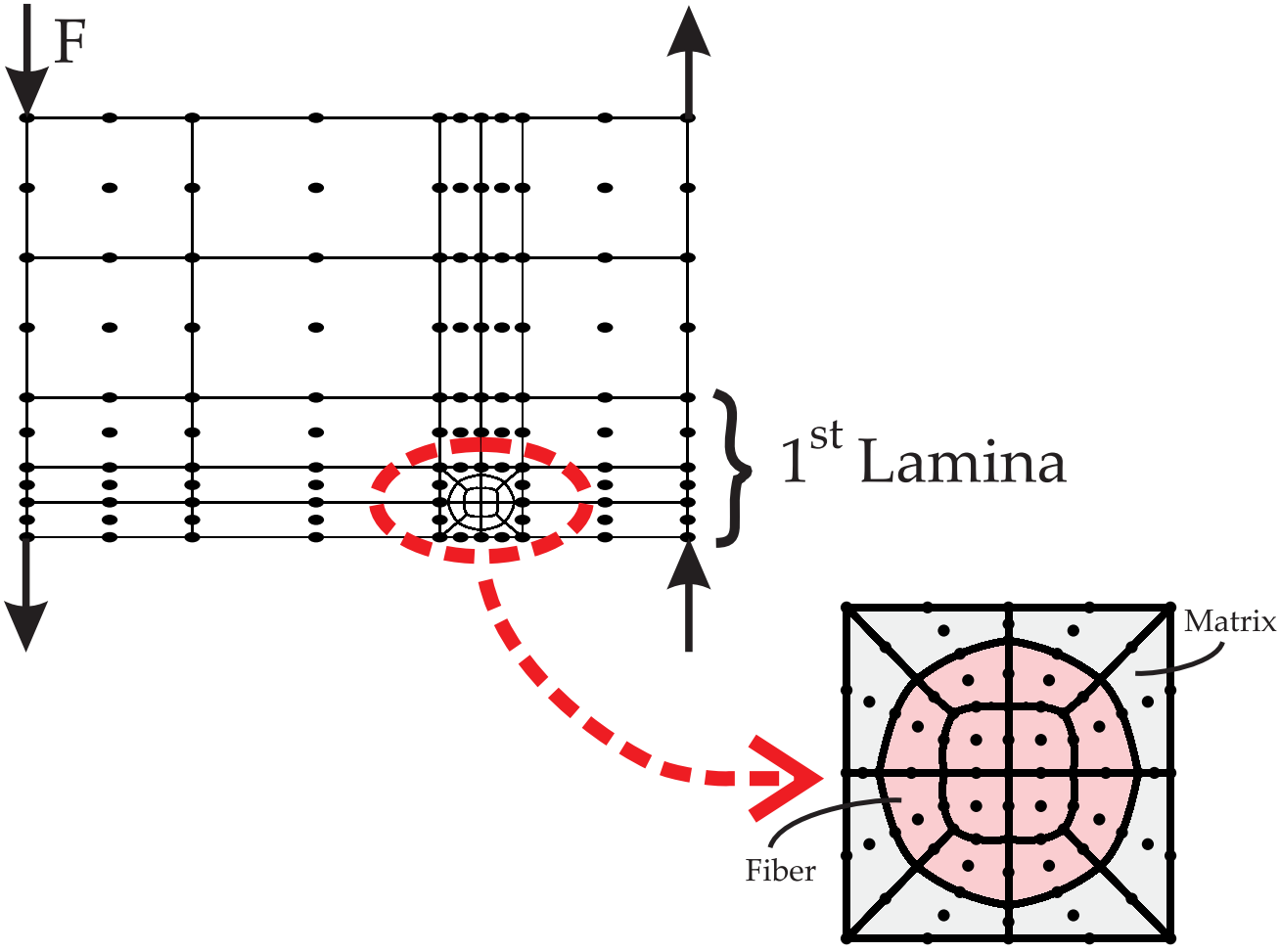

Figure 11. Laminate beam structure under torsion loading.

whole cell. Also in this case, concerning the bending load, the fiber is the component related to the axial strain energy while the matrix that related to the shear strain energy absorption. When subjected to torsional load the fiber absorbs the 99,2 % of the cell while the 88,3% of the shear energy is absorbed by the matrix. Evaluations of the FI* for the maximum stress criteria are provided for the fiber/matrix cell in Table 10. Through the CW approach, in a realistic structural configuration failure parameters can be evaluated on components properly refining the model.

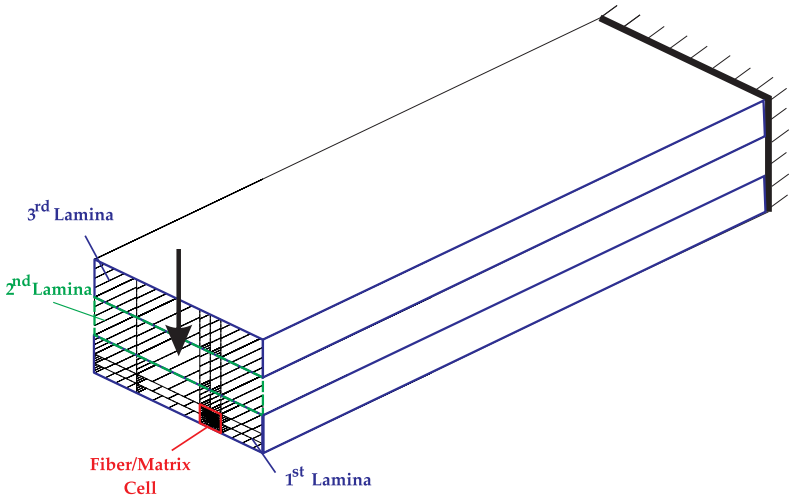

Figure 12. Laminated beam model.

	Bending			Torsion		
	E_i/E	$E_{ax,i}/E_{ax}$	$E_{s,i}/E_s$	E_i/E	$E_{ax,i}/E_{ax}$	$E_{s,i}/E_s$
Matrix	0.026	0.015	0.741	0.875	0.008	0.883
Fiber	0.974	0.985	0.259	0.125	0.992	0.117
	E [mJ]	E_{ax} [mJ]	E_s [mJ]	E [mJ]	E_{ax} [mJ]	E_s [mJ]
Cell	2.322×10^2	2.289×10^2	3.432×10^4	2.582×10^3	2.977×10^5	2.515×10^3

Table 9. Strain energy distribution in a fiber/matrix cell included in a laminate beam under bending F = 5 N and torsion F = 1 N loads.

FI* - MS		
	Bending	Torsion
Matrix	0.055	0.147
Fiber	0.266	0.190
Cell	0.182	0.173

Table 10. MS Failure index integrated over the fiber,matrix and whole cell subvolumes under bending F = 5 N and torsion F = 1 N loads.

VII. Conclusion

Different structural models have been discussed in this paper for the analysis of composite structures. The results were evaluated in terms of strain energy, failure index and a failure parameter FI^*.
Comparison with solid model results was provided for the homogeneous case study. Particular attention was given to a simple fiber-matrix cell unit in order to highlight the analysis capabilities of the formulation proposed. Then a more complex configuration was taken into account. The CW formulation, derived through 1D CUF structural models, can be used to model laminates, laminae, fibers and matrices separately, that is, different scale components can be modeled by using the same 1D formulation. Cells can be opportunely included in real configurations in order to refine the model in areas that, following preliminary analyses, were considered critical. Numerical results suggest that:

- Preliminary analyses lead to the identification of the areas of the structure where a model refinement is necessary. As a general guideline, to save computational cost the CW approach should be adopted where

results from macroscale models suggest to enrich the model. Identified these areas, refined models can be employed to obtain accurate stress/strain fields.

- Because of the solid like accuracy of the stress/strain distribution, effects due to local loads are captured by the model;
- Results highlight how the criticality of volumes strongly depend on the load conditions.
- Integral evaluations can be obtained at microscale level up to subvolumes of the components (fiber/matrix) with solid like accuracy. This approach can lead to progressively evaluate the criticality of the component and to detect failure location.

References

[1]Lu, G. and Kaxiras, E., *Handbook of Theoretical and Computational Nanotechnology*, Vol. X, American Scientific Publishers, 2005.

[2]Aboudi, J., *Mechanics of Composite Materials: A Unified Micromechanical Approach*, Elsevier, 1991.

[3]Aboudi, J., "Micromechanical Analysis of Thermo-lnelastic Multiphase Short-Fiber Composites," *Composites Engineering*, 1994, pp. 839–850.

[4]Pineda, E., Waas, A., Bednarcyk, B., Collier, C., and P.W., Y., "Progressive damage and failure modeling in notchedlaminated fiber reinforced composites," *International Journal of Fracture*, Vol. 158, No. 2, 2009, pp. 125–143.

[5]Kant, T. and Manjunath, B. S., "Refined theories for composite and sandwich beams with C^0 finite elements," *Computers and Structures*, Vol. 33, No. 3, 1989, pp. 755–764.

[6]Kapania, K. and Raciti, S., "Recent Advances in Analysis of Laminated Beams and Plates, Part I: Shear Effects and Buckling," *AIAA Journal*, Vol. 27, No. 7, 1989, pp. 923–935.

[7]Lekhnitskii, S., "Strength calculation of composite beams," *Vestnik inzhen i tekhnikov*, Vol. 9, 1935.

[8]Ambartsumian, S., "Contributions to the theory of anisotropic layered shells," *Applied Mechanics Review*, Vol. 15, 1962, pp. 245–249.

[9]Reissner, E., "On a certain mixed variational theory and a proposed application," *International Journal of Numerical Methods in Engineering*, Vol. 20, 1984, pp. 1366–1368.

[10]Carrera, E., "Historical review of Zig-Zag theories for multilayered plates and shells," *Applied Mechanics Review*, Vol. 56, No. 3, 2003, pp. 287–308.

[11]Robbins Jr., D. and Reddy, J., "Modeling of thick composites using a layer-wise theory," *International Journal of Numerical Methods in Engineering*, Vol. 36, 1993, pp. 655–677.

[12]Carrera, E., "Evaluation of layer-wise mixed theories for laminated plates analysis," *AIAA Journal*, Vol. 36, 1998, pp. 830–839.

[13]Carrera, E. and Petrolo, M., "Refined One-Dimensional Formulations for Laminated Structure Analysis," *AIAA Journal*, Vol. 50, 2012, pp. 176–189.

[14]Mourad, H., Williams, T., and Addessio, F., "Finite element analysis of inelastic laminated plates using a global-local formulation with delamination," *Comput. Methods Appl. Mech. Engrg.*, Vol. 198, 2008, pp. 542–554.

[15]Ben Dhia, H. and Rateau, G., "The Arlequin method as a flexible engineering design tool," *International Journal of Numerical Methods in Engineering*, Vol. 62, No. 11, 2005, pp. 1442–1462.

[16]Biscani, F. Giunta, G. B. S. C. E. and Hu, H., "Variable kinematic beam elements coupled via Arlequin method," *Composite Structures*, Vol. 93, No. 2, 2011, pp. 697–708.

[17]Biscani, F. Giunta, G. B. S. F. H. H. and Carrera, E., "Variable kinematic plate elements coupled via Arlequin method," *International Journal for Numerical Methods in Engineering*, 2012.

[18]Carrera, E., Maiaru, M., and Petrolo, M., "Component-wise analysis of laminated anisotropic composites," *International Journal of Solids and Structures*, Vol. 49, No. 13, 2012, pp. 1839–1851.

[19]Nali, P. and Carrera, E., "A numerical assessment on two-dimensional failure criteria for composite layered structures," *Composites: Part B*, Vol. 43, 2012, pp. 280–289.

[20]Orifici, A., Herszberg, I., and Thomson, R., "Review of methodologies for composite material modelling incorporating failure," *Composite Structures*, Vol. 86, 2008, pp. 194–210.

[21]Puck, A. and Schuermann, H., "Failure analysis of FRP laminates by means of physically based phenomenological models," *Composites Science and Technology*, Vol. 62 (1213), 2002, pp. 1633–62.

[22]Dávila, C. and Camanho, P. P., "Failure Criteria for FRP Laminates in Plane Stress," *NASA/TM-2003-212663*, 2003.

[23]Pinho, S. T., Dávila, C., Camanho, P. P., Iannucci, L., and Robinson, P., "Failure Models and Criteria for FRP Under In-Plane or Three-Dimensional Stress States including Shear Non-Linearity," *NASA/TM-2005-213530*, 2005.

[24]Reddy, J. N., *Mechanics of laminated composite plates and shells. Theory and Analysis*, CRC Press, 2nd ed., 2004.

[25]Carrera, E., Giunta, G., Nali, P., and Petrolo, M., "Refined beam elements with arbitrary cross-section geometries," *Computers and Structures*, Vol. 88, No. 5–6, 2010, pp. 283–293, DOI: 10.1016/j.compstruc.2009.11.002.

[26]Oñate, E., *Structural Analysis with the Finite Element Method: Linear Statics, Volume 1*, Springer, 2009.

[27]Bathe, K., *Finite element procedure*, Prentice hall, 1996.

[28]Carrera, E., Maiaru, M., and Petrolo, M., "A Refined 1D element for structural analysis of single and multiple fiber/matrix cells," *Composite Structures*, Vol. 96, 2013, pp. 455–468.